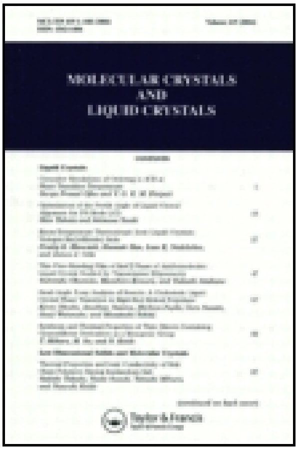

Molecular Crystals and Liquid Crystals

Publication details, including instructions for authors and subscription information:
http://www.tandfonline.com/loi/gmcl20

Organic Thin Film Photo-Transistors Based on Pentacene

Bruno Lucas [a] , Aumeur El Amrani [a] & André Moliton [a]

[a] Université de Limoges, Faculté des Sciences et Techniques, CNRS, Institut de Recherche XLIM, Département MINACOM, LIMOGES, France

Version of record first published: 31 Aug 2012.

To cite this article: Bruno Lucas , Aumeur El Amrani & André Moliton (2008): Organic Thin Film Photo-Transistors Based on Pentacene, Molecular Crystals and Liquid Crystals, 485:1, 955-964

To link to this article: http://dx.doi.org/10.1080/15421400801925885

Mol. Cryst. Liq. Cryst., Vol. 485, pp. 207/[955]–216/[964], 2008

ISSN: 1542-1406 print/1563-5287 online
DOI: 10.1080/15421400801925885

Organic Thin Film Photo-Transistors Based on Pentacene

Bruno Lucas, Aumeur El Amrani, and André Moliton
Université de Limoges, Faculté des Sciences et Techniques,
CNRS, Institut de Recherche XLIM, Département MINACOM,
LIMOGES, France

In this article, we studied the influence of light exposure on the electrical properties of a pentacene-based transistor. While the charge carrier mobility is found unaffected at $2.10^{-2} cm^2 V^{-1} s^{-1}$ after 2 hours of constant ultraviolet illumination, the photo-excitation mainly perturbs the charge carrier density in the active region. Irreversible change of the mobility was only observable after 10 hours of light exposure. The corresponding phototransistor performance under UV show a maximal current gain ($I_{dsillumination}/I_{dsdark}$) at $Vgs = 0V$ of 10^3. Moreover, light intensity dependent measurements revealed both a photovoltaic (in turn-on state) and a photoconductive (in turn-off state) effect in the device.

Keywords: organic transistor; pentacene; photoconductivity; phototransistor; UV illumination

1. INTRODUCTION

Today, thin film organic transistors (OTFTs) have similar performances than those associated with a-Si:H TFT [1]. The regular improvements of organic materials allow the use of these OTFTs in various applications, such as toggle switches in electronic circuits, memories for intelligent packaging or RFID in logical circuits, as well as phototransistors in active matrix or flat-screen displays [2–4]. For this last application, the device can be driven by light to act as switch in amplifiers, detection circuits or sensors of ultra sensitive image. The active component is then an OTFT that uses the photoconduction properties of the transistor active layer.

Address correspondence to Bruno Lucas, Université de Limoges, Faculté des Sciences et Techniques, CNRS, UMR 6172, Institut de Recherche XLIM, Département MINACOM, 123 Avenue Albert Thomas, 87060 Limoges, France. E-mail: bruno.lucas@unilim.fr

In this article, we present a study on the electrical behaviour of transistors based on pentacene in the dark and under light exposure. The performances of the phototransistor in term of mobility in the saturation regime, of threshold voltage, and of stability under ultraviolet (UV) illumination at 365 nm and under ambient atmosphere are presented and discussed. Moreover, we examine the influence of light intensity on the electrical properties of the OTFT in order to evidence additional functioning modes of the component such as photovoltaic or photoconductive effects.

2. EXPERIMENTALS

Pentacene based thin film (50 nm) transistors were deposited in "top-contact" geometry on indium tin oxide (ITO)-coated glass substrates using a 1 μm thick poly-(methyl-methacrylate) (PMMA) gate insulator (Fig. 1). The ITO substrates were prepared by ion beam sputtering [5] and the PMMA layer was deposited by spin-coating on the ITO gate electrode followed by an annealing step at 165°C for one hour. The pentacene film was obtained by vacuum evaporation with a deposition rate of 6 nm/min, without heating the substrate. The drain and source electrodes consist of gold thin layers (of about 50 nm) deposited by evaporation through a shadow mask defining a 50 μm long and 4 mm wide channel. All the devices were tested at room temperature and in ambient atmosphere.

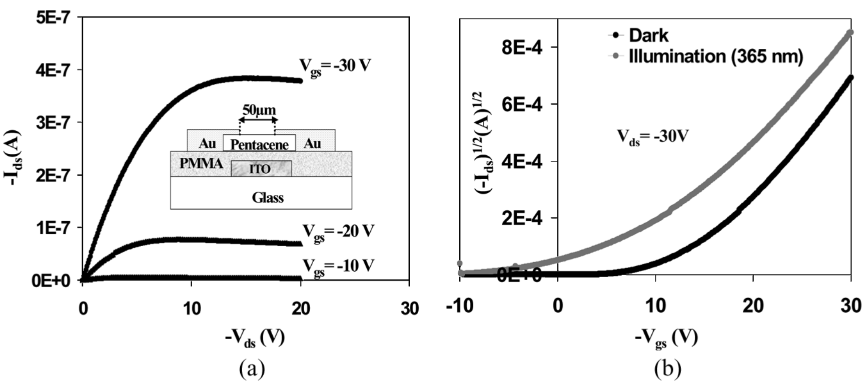

FIGURE 1 (a) $I_{ds} - V_{ds}$ curves obtained with a pentacene-based TFT in the dark for $V_{gs} = -10$, -20 and -30 V. In the inset: Schematic cross section of an organic thin film transistor. (b) $\sqrt{-I_{ds}} - V_{gs}$ transfer characteristics at $V_{ds} = -30$ V, of a pentacene-based TFT in the dark and under illumination at 365 nm.

The electrical characteristics of the transistors were recorded using a computer-controlled 4200 SMU Keithley source meter unit. The capacitance of the dielectric layer was measured with a RLC impedance analyser (HP 4284 A) between 20 Hz and 1 MHz. An ultraviolet lamp (model B 100 AP UVP with emission centred at 365 nm and with a power of 7 mW/cm^2) located at a distance of 25 cm from the transistor active layer was used to irradiate the device from the top (top electrodes side). The characterizations of the OTFTs under various light intensities were performed using a solar simulator (AM1.5) with intensities varying from 17 mW/cm^2 to 96 mW/cm^2 by using neutral density filters.

As far as the structural characterizations of pentacene were concerned, an atomic force microscope (AFM) and a Siemens D5000 diffractometer ($\lambda = 1.54$ nm) for X-ray diffraction measurements were used. The absorption spectra were obtained with a UV-visible-near infra-red spectrophotometer covering the 200 nm–1200 nm wavelength range.

3. ELECTRICAL CHARACTERIZATIONS OF AN ORGANIC THIN FILM TRANSISTOR (OTFT) IN THE DARK AND UNDER OPTICAL EXCITATION AT 365 nm

The output characteristic $I_{ds} = f(V_{ds})$ of the OTFT is given in Figure 1a for various gate bias voltages from -10 V to -30 V: when V_{gs} increases, a field effect is obtained with a maximum on/off ratio (I_{on}/I_{off}) of about $1.5 \cdot 10^5$ in the ON state ($I_{on} = 3.8 \cdot 10^{-7}$A and $I_{off} = 2.5 \cdot 10^{12}$ A at $V_{gs} = -30$ V). We also present the plot of $\sqrt{-I_{ds}} = f(V_{gs})$ at $V_{ds} = -30$ V (Fig. 1b) to determine the charge carrier mobility (μ) in the saturation regime which follows the equation suggested by reference [6]: $I_{ds}^{sat} = WC_i\mu/2L(V_{gs} - V_T)^2$ where L and W are the length and the width of the channel respectively, C_i is the insulator capacitance per surface unit ($C_i = 2.3$ nF/cm^2 for 1 μm of PMMA and $\varepsilon \approx 2.6$) and V_T is the threshold voltage. The values obtained in the dark for the mobility and the threshold voltage are 0.02 cm^2 V^{-1} s^{-1} and 14 V respectively. Besides, when we expose the phototransistor under UV light at 365 nm from the semiconductor side ("on-top" illumination), a primary photocurrent appears (Fig. 1b). This current is due to the photogeneration of electron-hole pairs in the channel. Figure 1b shows, on one hand, a strong increase in the drain current under UV irradiation due to the additional photogenerated carriers, and, on the other hand, a decrease in the threshold voltage indicating that the charge carrier density in the channel is reinforced by photodopage. If we evaluate the increase in the charge carriers per surface unit due to UV exposure using the relation $\Delta N = C_i \Delta V_T / e$ where C_i is the capacitance per surface unit of the dielectric layer, e is the elementary charge and $\Delta V_T = 6.5\,V$ corresponds to the difference of the threshold voltage in the dark ($V_T = 14\,V$) and under UV ($V_T = 7.5\,V$), we obtain $\Delta N \approx 10^{11} cm^{-2}$. We note that the mobility is not modified under UV (around $2.10^{-2} cm^2/V^{-1} s^{-1}$) since the slopes in the representation $\sqrt{-I_{ds}} = f(V_{gs})$ are similar in the dark and under UV. Moreover, the ratio between the current under illumination and in the dark gives a maximum current gain of about $2.3 \cdot 10^3$ at $V_{gs} = -2.8\,V$ and around 10^3 at $V_{gs} = 0\,V$ (Fig. 2). When one of the two gates is turned off (for $V_{gs} = 0\,V$ or without light excitation), the effect of the other gate is maximized. For example, on one hand, the on/off ratio is much higher at $V_{gs} = -30\,V$ without illumination ($I_{on}/I_{off} = 1.5 \cdot 10^5$ in the dark and $I_{on}/I_{off} = 300$ under illumination) and, on the other hand, the ratio $I_{dsillumination}/I_{dsdark}$ in the accumulation regime is much lower than the one obtained at $V_{gs} = 0\,V$. This indicates that a gate voltage applied in the accumulation regime is inefficient to induce a high photoresponse. Consequently, these results show that the transistor with two electrodes (drain and source) can act as a photodetector as well as a current amplifier under illumination.

Before considering this organic device in a particular application, it is important to evaluate its stability under ambient atmosphere and during a continuous exposure to UV irradiation. As most organic materials, pentacene is sensitive to environmental conditions and can be degraded under UV. Thus, we first represented the transfer

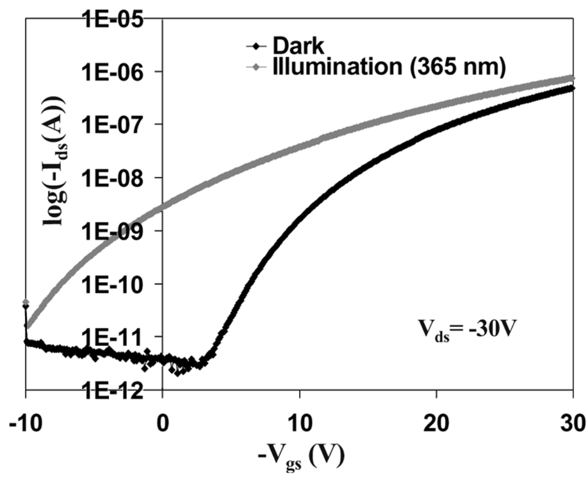

FIGURE 2 $\log(I_{ds}) - V_{gs}$ curves at $V_{ds} = -30\,V$ of a pentacene-based TFT in the dark and under illumination at 365 nm.

characteristics of a transistor continuously tested in the dark during approximately 24 hours (Fig. 3a). The charge carrier mobility remains unchanged on this timescale, and only the charge carrier density increases significantly due to the presence of ambient oxygen that causes a doping of the pentacene and affects its conduction properties. Then, we plot the transfer characteristics of a transistor continuously tested under UV irradiation during approximately 24 hours (Fig. 3b). Under irradiation, two effects are observable: on one hand, an increase in the carrier density and on the other hand, a significant decrease of the mobility after 12 hours of continuous exposure to UV radiations from 1.5 $10^{-2} cm^2 V^{-1} s^{-1}$ down to 5 $10^{-4} cm^2 V^{-1} s^{-1}$. After 12 hours of light exposure, this value remains constant. When finally switching the light excitation off, the initial transfer characteristic of the photo-transistor in the dark is not recovered 24 hours later. The mobility is divided by an order of magnitude compared to its initial value; this decay is attributed to a partial degradation of the polycrystalline pentacene structure under 365 nm UV illumination. To underscore this degradation, we carried out AFM, X-ray diffraction and absorption spectroscopy measurements for pentacene films in their pristine state and after 24-hour UV exposure in air.

AFM patterns (2 μm × 2 μm) were realized on 50 nm thick pentacene layers deposited on 1μm of PMMA spin-coated on an ITO substrate (Fig. 4). Figure 4a presents the pentacene structure in its pristine state, we can observe clusters of dendritic grains well-connected

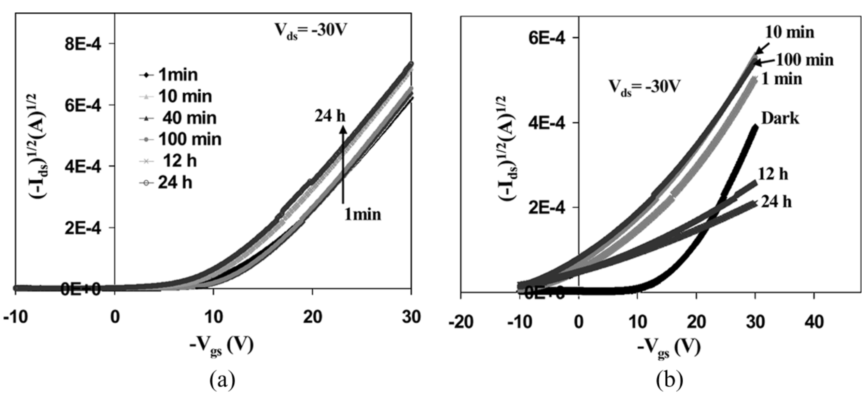

FIGURE 3 (a) $\sqrt{-I_{ds}} - V_{gs}$ transfer characteristics at $V_{ds} = -30\,V$, obtained for a pentacene-based TFT continuously tested in the dark (for times varying between 1 min and 24 h). (b) $\sqrt{-I_{ds}} - V_{gs}$ transfer characteristics at $V_{ds} = -30\,V$ of a pentacene-based TFT continuously tested under UV irradiation (for times varying between 1 min and 24 h).

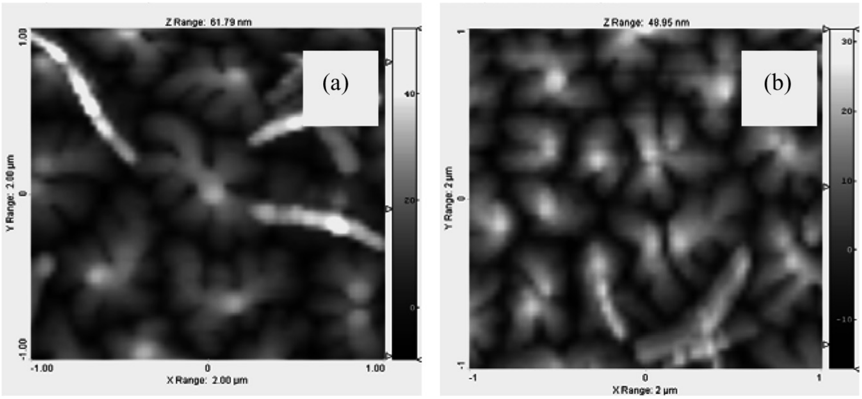

FIGURE 4 (a) AFM pattern (2μm × 2μm) for a 50 nm thick pentacene film on PMMA. (b) AFM pattern (2 μm × 2 μm) for a 50 nm thick pentacene film exposed to the UV (365 nm) light during 24 hours in air.

together. Figure 4b shows an AFM image of a pentacene layer irradiated during 24 hours under UV exposure; the layer morphology is different, grain clusters are smaller and the intergrain zones are wider and in great numbers after UV irradiation [7]. Thus it is not surprising that charge carrier mobility is weaker after the long-term UV exposure of pentacene films. The X-ray analysis (Fig. 5a) allows to check that the pentacene layers are well-organized and we find back diffraction plans [8] of the thin film phases. The thin film phase

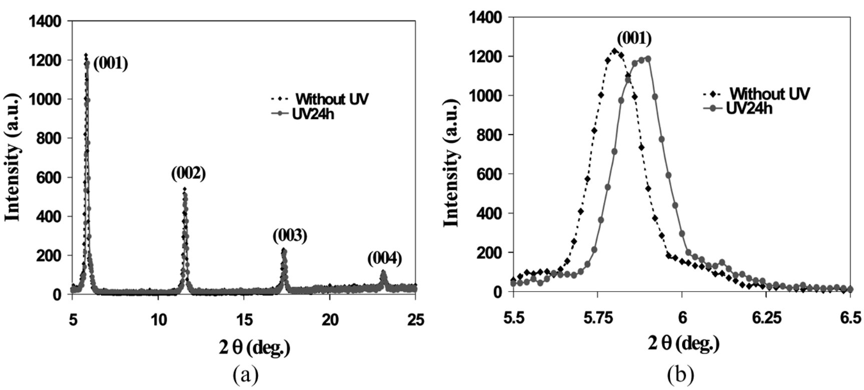

FIGURE 5 (a) X-ray diffraction of 50 nm thick pentacene films in their pristine state and under UV exposure during 24 hours in air. (b) Zoomed image of the peak assigned to the (001) plan reflection.

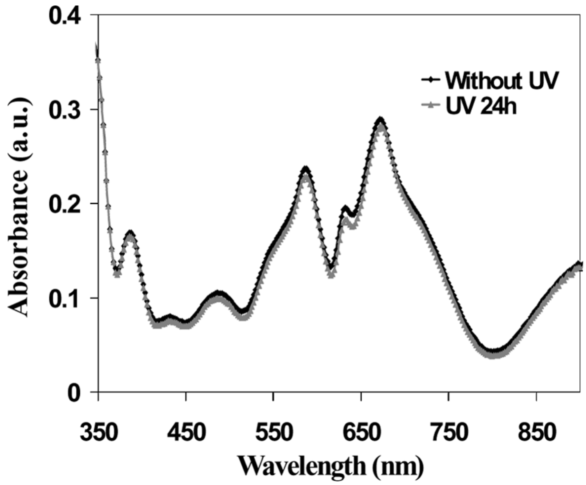

FIGURE 6 Absorption spectra of 50 nm thick pentacene films in their pristine state and under UV exposure during 24 hours in air.

presents an angle $2\theta = 5.8^\circ$ corresponding to an interplanar distance of 1.53 nm; the pentacene film is polycrystalline. Figure 5b shows a zoomed image of the peak assigned to the (001) plane reflection of a pristine pentacene film and irradiated by UV during 24 hours; we can note a shift diffraction peak towards the higher angles (or smaller interplanar distances) in the case of the UV irradiated film. This result can be explained by a compaction effect (already observed by other authors [9]) and it is in agreement with the AFM analysis. On Figure 6, we represented absorption spectra of non-irradiated and 24-hour irradiated pentacene films, it clearly appears that absorption peaks decrease in intensity after UV illumination (such as the absorption peak observed near 670 nm corresponding to the optical threshold for the highest occupied molecular orbital-lowest unoccupied molecular orbital). This decrease in absorption is related to the crystalline quality of the pentacene and can affect the charge transport as confirmed by our results of charge carrier mobility measurements; similar results were reported with other organic materials [10–11].

4. INFLUENCE OF LIGHT INTENSITY ON THE CHARACTERISTICS OF AN ORGANIC THIN FILM TRANSISTOR (OTFT)

In this part, the OTFT is exposed under simulated sunlight (AM1.5) at various light intensities varying from 17 mW/cm^2 to 96 mW/cm^2. The

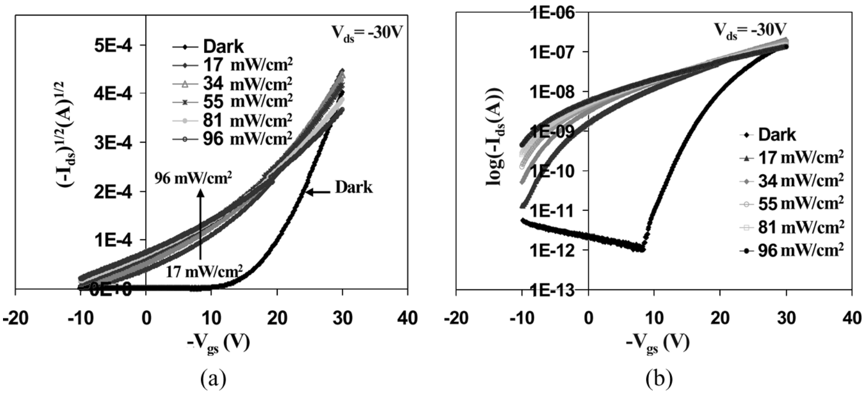

FIGURE 7 (a) $\sqrt{-I_{ds}} - V_{gs}$ transfer characteristics at $V_{ds} = -30\,V$ for a pentacene-based TFT in the dark and under various light intensities (varying between $17\,mW/cm^2$ and $96\,mW/cm^2$) (b) $\log(I_{ds}) - V_{gs}$ curves at $V_{ds} = -30\,V$ of a pentacene-based TFT in the dark and under various light intensities (varying between $17\,mW/cm^2$ and $96\,mW/cm^2$).

transfer characteristics of the device are presented Figure 7. On one hand, we observe that the mobility and threshold voltage decrease when the optical power increases (Fig. 7a), and on the other hand the photocurrent gain increases when the optical power increases (Fig. 7b). The last effect is more significant in the depletion regime (at $V_{gs} = 0\,V$, the photocurrent gain increases from 10^3 to $4 \cdot 10^3$ when light power increases from $17\,mW/cm^2$ to $96\,mW/cm^2$). When the photocurrent is presented versus light power (Fig. 8), two function modes [12,13] are underscored according to the polarization state of the transistor:

- a photovoltaic effect at the bounds of a Schottky junction in the accumulation regime ($V_{gs} = -15\,V$). This effect is due to accumulation and trapping of charges under the source electrode. It is described by the equation [14]: $I_{ph,pv} = G_M \Delta V_T = (AkT/q) \ln\left(1 + (\eta q \lambda P_{opt})/(I_{dark} hc)\right)$, where G_M is the transconductance, ΔV_T the threshold voltage shift, A is a fit parameter, η the quantum efficiency, P_{opt} the optical power, I_{dark} the dark current and hc/λ the photon energy. The decrease in the threshold voltage under illumination is attributed to the photovoltaic effect in which photogenerated electrons in the pentacene channel move near the source electrode and accumulates at the potential barrier between the source electrode and the active layer. This causes a change in the potential barrier for holes, leading to an increase in the

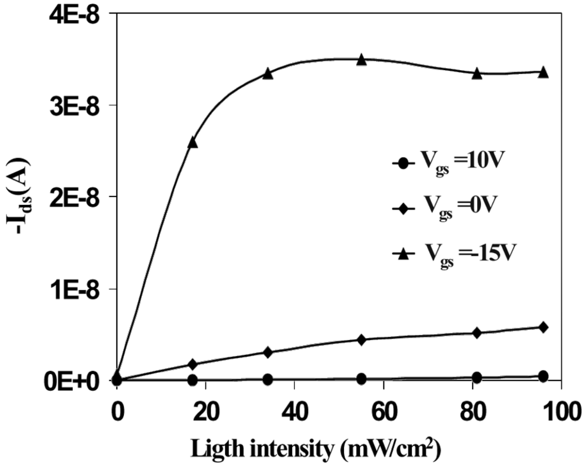

FIGURE 8 Photocurrent versus light intensity in on-state ($V_{gs} = -15\,V$) and in off-state ($V_{gs} = 0\,V$ and $V_{gs} = 10\,V$).

concentration of excess charge carriers and to a shift in the threshold voltage.

- a photoconductive effect in the depletion regime ($V_{gs} = 0\,V$ or $V_{gs} = 10\,V$). This effect is produced by the photogeneration of additional charges in the conductive channel. The number of these charges increases the drain current according to a linear law given by [15]: $I_{ph,pc} = (q\mu nE)WD = BP_{opt}$, where μ is the carrier mobility, n is the carrier density, E the electrical field, W the gate width, D the thickness of the active layer, and B and P_{opt} are a proportionality factor and the optical power respectively.

To summarise, the experimental results given on Figure 8 are in agreement with the two equations proposed in the ON- and OFF-state of the transistor.

5. CONCLUSIONS

Electrical characteristics of an organic pentacene-based transistor are analysed in the dark and under light exposure. We show that light can modify the charge carrier density and/or mobility. In the case of a continuous UV exposure (2 hours), the carrier density is mainly modified, whereas the associated mobility remains constant around $10^{-2}\,cm^2\,V^{-1}\,s^{-1}$ up to 10 hours exposure before irreversible effects arise. These effects, mainly due to the partial degradation of the polycrystalline pentacene structure (confirmed by optical absorption, X-ray diffraction and AFM measurements), lead to a strong decrease of the mobility measured in the dark 48 hours after the first measurement.

Performance of the phototransistor under illumination show a decrease of the threshold voltage and an increase of the current gain ($I_{dsillumination}/I_{dsdark}$) at $V_{gs} = 0\,V$ from 10^3 to 4.10^3 for an incident light power density from 17 to 96 mW/cm^2. Moreover, two additional effects are evidenced depending on the transistor polarization state: a photovoltaic effect in the accumulation regime and a photoconductive effect in the depletion regime.

REFERENCES

[1] Jang, J. & Han, S. H. (2006). *Current Applied Physics*, *6S1*, e17.
[2] Noh, Y.-Y., Yase, K., & Kim, D.-Y. (2005). *J. Appl. Phys.*, *98*, 074505.
[3] Hu, Y., Dong, G., Liu, C., Wang, L., & Qiu, Y. (2006). *Appl. Phys. Lett.*, *89*, 072108.
[4] Marjanović, N., Singh, B., Dennler, G., Günes, S., Neugebauer, H., Sariciftci, N. S., Schwödiauer, R., & Bauer., S. (2006). *Org. Electron.*, *7*, 188.
[5] Lucas, B., Rammal, W., & Moliton, A. (2006). *Eur. Phys. J. Appl. Phys.*, *34*, 179–187.
[6] Horowitz, G. (1999). *J. Matter. Chem.*, *9*, 2001.
[7] Vollmer, A., Jurchescu, O. D., Arfaoui, I., Salzmann, I., Palstra, T. T. M., Rudolf, P., Niemax, J., Pflaum, J., Rabe, J. P., & Koch, N. (2005). *Eur. Phys. J.*, *17*, 339.
[8] Shtein, M., Mapel, J., Benziger, J. B., & Forrest, S. R. (2002). *Appl. Phys.*, *81*, 268.
[9] Kim, W. J., Koo, W. H., Jo, S. J., Kim, C. S., Baik, H. K., Hwang, D. K., Lee, K., Kim, J. H. & Im, S. (2006). Electrochem. *Solid-State Lett.*, *9*, 251.
[10] Ficker, J., von Seggem, H., Rost, H., Fix, W., Clemens, W., & McCulloch, I. (2004). *Appl. Phys. Lett.*, *85*, 1377.
[11] Choi, J. M., Hwang, D. K., Hwang, J. M., Kim, J. H., & Im, S. (2007). *Appl. Phys. Lett.*, *90*, 113515.
[12] Takanashi, Y., Takahata, K., & Muramoto, Y. (1998). *IEEE Electron Device Letters*, *19*, 472.
[13] Marjanovic, N., Singh, Th. B., Dennler, G., Günes, S., Neugebauer, H., Sariciftci, N. S., Schwödiauer, R., & Bauer, S. (2006). *Organic Electronics*, *7*, 188.
[14] Kang, H. S., Choi, C. S., Choi, W. Y., Kim, D. H., & Seo, K. W. (2004). *Appl. Phys. Lett.*, *84*, 3780.
[15] Sze, S. M. (1981). *Physics of Semiconductor Devices*, Wiley: New York.